Published in final edited form as:
Nat Cell Biol. 2012 August ; 14(8): 851–858. doi:10.1038/ncb2529.

Direct inhibition of the cold-activated TRPM8 ion channel by $G\alpha_q$

Xuming Zhang[1], **Stephanie Mak**[1], **Lin Li**[1], **Andres Parra**[2], **Bristol Denlinger**[2], **Carlos Belmonte**[2], and **Peter A. McNaughton**[1]

[1]Department of Pharmacology, University of Cambridge, Tennis Court Road, Cambridge, CB2 1PD, United Kingdom

[2]Instituto de Neuroscience de Alicante, Universidad Miguel Hernandez-Consejo Superior de Investigaciones Cientificas, 03550 San Juan de Alicante, Spain

Abstract

Activation of the TRPM8 ion channel in sensory nerve endings produces a sensation of pleasant coolness. Here we show that inflammatory mediators such as bradykinin and histamine inhibit TRPM8 in intact sensory nerves, but do not do so via conventional signalling pathways. The G-protein subunit $G\alpha_q$ instead binds to TRPM8 and when activated by a Gq-coupled receptor directly inhibits ion channel activity. Deletion of $G\alpha_q$ largely abolished inhibition of TRPM8, and inhibition was rescued by a $G\alpha_q$ chimera whose ability to activate downstream signalling pathways was completely ablated. Activated $G\alpha_q$ protein, but not $G\beta\gamma$, potently inhibits TRPM8 in excised patches. We conclude that $G\alpha_q$ pre-forms a complex with TRPM8 and inhibits activation of TRPM8, following activation of G-protein coupled receptors, by a direct action. This signalling mechanism may underlie the abnormal cold sensation caused by inflammation.

Keywords

pain; TRPM8; G proteins; GPCR; inflammatory mediators; sensory transduction

The temperature sensitive ion channels TRPV1 and TRPM8 play an essential role in the pain pathway. Inflammatory mediators released during tissue injury or inflammation enhance heat pain by sensitizing the heat-gated TRPV1 ion channel via intracellular signalling pathways whose endpoint is phosphorylation of TRPV1 by protein kinases[1-5]. The TRPM8 ion channel is activated by cold temperatures[6, 7], and is also involved in many aspects of pain sensation such as cold analgesia, and paradoxically cold hypersensitivity[8-12]. Acute activation of TRPM8, by cooling or by application of agonists of TRPM8 such as menthol, causes an analgesic effect[8, 9]. Cold hypersensitivity, on the other hand, is observed in chronic inflammatory conditions, and increased TRPM8 expression appears to be an underlying mechanism[8, 10, 13]. It is thus unclear how TRPM8-expressing cold thermoreceptors may be affected by inflammation.

The membrane PIP_2 level reulates TRPM8 activity. TRPM8 activity increased when PIP_2 was applied to the intracellular surface of excised patches[14, 15], and was reduced when membrane PIP_2 was depleted[16]. A decrease in membrane PIP_2, caused by activation of the

Correspondence should be addressed to X.Z. or P.A.M. (xz213@cam.ac.ukorpam42@cam.ac.uk) .

AUTHOR CONTRIBUTIONS X.Z. came up with the hypothesis, designed and performed experiments, and analysed data except calcium imaging experiments, which were carried out by S.M., and nerve fibre recordings which were carried out by A.P, B.D., C.B. and P.A.M.; L.L. assisted with molecular biology experiments and neurons preparation. X.Z. wrote the manuscript with input from C.B. and P.A.M. X.Z. and P.A.M. supervised the project.

Europe PMC Funders Author Manuscripts

PLC pathway following binding of an agonist such as bradykinin (BK) to a Gq-coupled GPCR, was therefore assumed to be responsible for inhibiting TRPM8 channel activity[14, 15]. However, other studies have proposed that PKC is instead involved in the inhibition of TRPM8 by BK[17, 18].

In the present study we examined the effect of inflammatory mediators on TRPM8-dependent nerve activity, and we confirm that TRPM8 is inhibited by inflammatory mediators which couple to $G\alpha_q$. However, we found that the inhibition of TRPM8 activity is largely independent of cell signalling pathways downstream of $G\alpha_q$-coupled receptors. Neither depletion of membrane PIP_2 nor phosphorylation by PKC is crucial. Instead we found that activated $G\alpha_q$ binds to TRPM8, and causes inhibition by a direct action following activation of $G\alpha_q$-coupled receptors.

RESULTS

Inflammation inhibits TRPM8-dependent cold nerve fibre activity

Cold-sensitive fibres innervating the cornea of the eye detect small changes in ambient cold temperature, a property solely dependent on TRPM8 channel expression[19]. We first examined the effect of inflammatory mediators on cold-sensitive fibres of the cornea. A cooling ramp from 34°C to 20°C elicited an increasing discharge of nerve impulses (Fig. 1a), known to be attributable to activation of TRPM8[19]. A heat ramp to 48°C initially suppressed ongoing TRPM8-dependent activity, but then reactivated firing at 45°C, likely because of heat–dependent activation of TRPV1. However, when an “inflammatory soup” (IS), containing BK and histamine was perfused, increases in firing frequency evoked by cooling were smaller (grey arrows in Fig. 1a, mean peak frequency before IS, 44.3±4.5 impulses per second; after IS, 31.8±3.4; n=12, $P<0.001$, paired *t* test). A significantly larger temperature decrease (ΔT) for initiation of increased firing was also observed (ΔT before IS, 1.1±0.4°C; after IS, 1.8±0.4°C; n=12, $P<0.01$, paired *t* test). In contrast, the firing frequency evoked by heat was enhanced by inflammatory mediators (black arrows, Fig. 1a). We found no significant desensitization of firing frequency under control condition when saline solution was perfused (mean peak frequency before saline solution, 47.5±5.95 impulses per second; after saline, 44.0±7.7; n=4, $P>0.05$, paired *t* test; Supplementary Fig. S1a)[19]. These data show that inflammatory agents suppress TRPM8-mediated responses to cooling in intact cold thermoreceptor terminals *in situ*, while at the same time enhancing heat responses.

A similar result in cold-sensitive afferent nerve fibres of the mouse tongue was obtained when inflammation was induced by carrageenan injection. Fig. 1b shows the cumulative sum of firing in single sensory afferent nerves as the temperature was lowered from 34°C to 12°C; the integral of firing as a function of temperature was half-activated at 31.6±1.09°C (n=40) in control fibres but at 25.4 ±0.81°C (n=32) in inflamed fibres.

Inflammatory mediators inhibit TRPM8 independent of conventional downstream signalling pathways

We next measured the activity of TRPM8 in cultured DRG neurons by applying pulses of menthol, an agonist for TRPM8, and monitoring the rise in $[Ca]_i$ caused by channel activation. In agreement with nerve fibre recordings, BK potently inhibited TRPM8 in 11 out of 33 TRPM8 positive neurons (Fig. 2a). PKC-mediated phosphorylation, either direct or via activation of a phosphatase, has been suggested to be responsible for inhibition of TRPM8[17, 18], but we found that the BK-induced inhibition of TRPM8 was not abolished by the PKC inhibitor BIM, and nor was it mimicked by the PKC activator PMA (Fig. 2b; Supplementary Fig. S1b,c). Similar observations were made in HEK293 cells co-transfected

with TRPM8 and the BK receptor B2R, in which BK inhibited TRPM8 with a similar efficacy to DRG neurons (Fig. 2c,d; Supplementary Fig. S1d). B2R-dependent inhibition of TRPM8 was not affected by the specific PKC inhibitor BIM, nor by the broad PKC inhibitor staurosporine, the phosphatase inhibitor okadaic acid, nor the PLC inhibitor neomycin (Fig. 2d). Moreover, activation of PKC by PMA did not cause significant inhibition of TRPM8 (Fig. 2d), though PMA had a marked effect on TRPV1 (Supplementary Fig. S1e). These experiments do not favour the idea that signalling pathways downstream of PLC may underlie the effect of BK on TRPM8.

To extend these experiments, the current flowing through TRPM8 channels was monitored during voltage-clamp pulses to ±60mV or in full I-V curves (Supplementary Fig. S2a,b), and the effects of inhibitors on signalling pathways were investigated. Membrane PIP_2 is known to activate TRPM8[14, 15], and therefore PIP_2 hydrolysis following activation of PLCβ by G_q-coupled GPCRs could be a mechanism for inhibiting TRPM8. This idea is not supported, however by the inability of U73122, a PLC inhibitor, to prevent the inhibition of TRPM8 currents (either inward or outward) caused by BK or histamine (Fig. 2e-h). The same concentration of U73122 completely inhibited PLC-mediated hydrolysis of PIP_2 and also inhibited the sensitization of TRPV1 induced by BK (Supplementary Fig. S3a,b), a process dependent on the PLC signalling pathway[5, 20].

Moreover, histamine strongly inhibited TRPM8 currents in two PIP_2-insensitive TRPM8 mutants, K995Q and R1008Q[14] (Fig. 2g, h). We also found that activation of PLCγ via application of NGF had no inhibitory effect on TRPM8 (Fig. 2d, last bar). These experiments suggest that receptor-mediated hydrolysis of PIP_2 is not sufficient to inhibit TRPM8. A possible pathway involving activation of PLA_2 followed by coupling to $G\alpha_i$ is also not supported by the lack of effect of the PLA_2 inhibitor ACA and inactivation of $G\alpha_{i/o}$ by PTX (Fig. 2e,f). Disruption of intracellular Ca^{2+} signalling by applying the Ca uptake inhibitor thapsigargin, by buffering intracellular calcium with BAPTA-AM or by blocking the IP3 receptor with 2-APB also had no effect on BK-induced inhibition of TRPM8 currents, suggesting that intracellular Ca^{2+} release is not involved (Fig. 2f; Supplementary Fig. S1f).

Taken together, these data indicate that the conventional intracellular signalling pathways downstream of PLC are not involved in TRPM8 inhibition, and we therefore investigated other possible mechanisms.

Activated $G\alpha_q$ inhibits TRPM8 independent of the PLC pathway

Whether a diffusible intracellular mediator is involved in the inhibition of TRPM8 by BK can be determined by making cell-attached patch recordings of single channels and applying BK only outside the patch. Sensitization of TRPV1 depends on activation of kinases by the PLC signalling pathway[5], and as expected application of BK outside the patch potently enhanced channel activity (Fig. 3b). TRPM8 single channel bursting, by contrast, was not inhibited by bath application of BK (Fig. 3a). These experiments suggest that BK-induced inhibition of TRPM8 is membrane-delimited and depends on local events within the patch, and not on diffusible messengers.

The local nature of TRPM8 channel inhibition suggested that activated $G\alpha_q$ itself may cause direct inhibition of TRPM8, as previously suggested for K channels[21, 22]. $G\alpha_q$ has two forms, an inactive GDP-bound and an active GTP-bound form. Over-expression of $G\alpha_q$ had a small inhibitory effect on TRPM8 inward current (Fig. 4a), presumably because a small proportion of $G\alpha_q$ is in the active GTP-bound form even in the absence of GPCR stimulation[23]. The $G\alpha_{q/11}$ Q209L mutant, which is deficient in intrinsic GTPase activity and

is therefore mainly in the GTP-bound active configuration[24], caused a much greater inhibition of both inward and outward TRPM8 currents (Fig. 4a,b).

Inhibition of TRPM8 by active $G\alpha_q$ could result from potent activation of PLCβ, and consequent hydrolysis of PIP_2. To test this possibility, we used a sensitive reporter of membrane PIP_2 levels, Tubby-cYFP-R332H[25], to monitor activation of the PLCβ/PIP_2 pathway. As expected, expression of the active mutant $G\alpha_q$ Q209L, which couples to PLCβ, caused complete translocation of Tubby to the cytoplasm, while wild type $G\alpha_q$, which is largely in the inactive GDP-bound form, had no detectable effect (Supplementary Fig. S4a). A commonly used triple mutant $G\alpha_q$ Q209L/R256A/T257A, which has been reported to be unable to activate PLCβ[26], profoundly suppressed TRPM8 currents (Fig. 4b), but we found this mutant still caused substantial Tubby translocation (Supplementary Fig. S4a), and so in fact still couples to PLCβ. We therefore constructed a chimera between $G\alpha_q$ and $G\alpha_{i2}$ by replacing the PLCβ binding region on $G\alpha_q$, by the corresponding region on $G\alpha_{i2}$ (Fig. 6f). We found that this chimera, which we named $3G\alpha_{qiq}$ (see below), completely failed to deplete PIP_2 even when made constitutively active by the Q209L mutation (Supplementary Fig. S4a). However, when activated by the Q209L mutation, $3G\alpha_{qiq}$ strongly inhibited both inward and outward TRPM8 currents (Fig. 4a, b), showing that the $3G\alpha_{qiq}$ chimera retains the ability to couple to TRPM8, even though its coupling to PLCβ is selectively disabled. The inhibition of TRPM8 was specific to $G\alpha_q$, because other activated Gα subunits ($G\alpha_{i2}$ Q205L and $G\alpha_{13}$ Q226L) and $G\beta_1\gamma_2$ were without effect (Fig. 4b). Collectively, these experiments show that activated $G\alpha_q$ can directly inhibit TRPM8, independent of downstream PLC pathway.

The effect of $G\alpha_q$ on TRPM8 inward currents activated by menthol is shown in Fig. 4c. Over-expression of $G\alpha_q$ reduced TRPM8 sensitivity to menthol, because a small fraction is in the active GTP-bound conformation (see above). The constitutively active but signalling-ablated mutant 3G α_{qiq} Q209L caused a stronger inhibition of TRPM8 sensitivity to menthol. Conversely, expression of TRPM8 in MEF cells lacking endogenous Gα 27 q/11 , enhanced TRPM8 sensitivity to menthol, showing that endogenous $G\alpha_q$ imposes a tonic inhibition on TRPM8. Outward TRPM8 currents can be evoked by strong depolarization in either the absence or presence of menthol, and these currents were suppressed by $G\alpha_q$ and to an even greater extent by $3G\alpha_{qiq}$ Q209L, leading to a shift of the G-V curve and a significant positive shift in $V_{½}$ (Fig. 4d-f). We noticed that currents recorded in cells without menthol consistently have a larger noise than in the presence of menthol, presumably caused by a flickering opening of TRPM8 channels (see below Fig. 7a,b). These results show that TRPM8 activation, whether by menthol or by depolarization, is inhibited by active $G\alpha_q$ by shifting the voltage dependence of TRPM8 towards more positive membrane potentials. The strong inhibition caused by the signalling-ablated mutant $3G\alpha_{qiq}$ Q209L shows that inhibition occurs without engagement of downstream signalling pathways.

Inflammatory mediators inhibit TRPM8 via a direct action of activated $G\alpha_q$

To further investigate whether the coupling of the $3G\alpha_{qiq}$ chimera to PLCβ is completely disabled, we transfected the PIP_2 reporter Tubby-R332H-YFP along with the BK receptor into $G\alpha_{q/11}$-null MEF cells. Tubby rapidly translocated to the cytoplasm following BK treatment when wild type $G\alpha_q$ was co-transfected, but there was no translocation with the $3G\alpha_{qiq}$ chimera (Fig. 5a,b). Similar results were obtained with another PLCβ signalling reporter PLCδ-PH-EGFP (Supplementary Fig. S4b,c). These data indicate that the $3G\alpha_{qiq}$ chimera lacks the ability to activate PLCβ.

We then used the $3G\alpha_{qiq}$ chimera in gain-of-function experiments in the $G\alpha_{q/11}$-deficient MEF cells. Histamine caused no suppression of TRPM8 activity, confirming the complete deletion of $G\alpha_{q/11}$ in the MEF cells, but transfection of the $3G\alpha_{qiq}$ chimera rescued

suppression (Fig. 5c, d; Supplementary Fig. S2d). Similarly, the 3Gα_{qiq} chimera also rescued BK-mediated inhibition of TRPM8 currents (Fig. 5e, f; Supplementary Fig. S2c). The rescue of coupling from GPCRs to TRPM8 by 3Gα_{qiq}, which is unable to couple to PLCβ, confirms that Gα_q couples directly to TRPM8 without the need to involve signalling pathways downstream of PLC.

Gα_q binds directly to TRPM8

Direct modulation of TRPM8 by Gα_q suggests that they might form a complex. Fig. 6a shows that both wild-type Gα_q and active Gα_q Q209L were pulled down by TRPM8 to a similar extent. Reciprocally, TRPM8 was co-precipitated by either Gα_q or Gα_q Q209L (Fig. 6b). Co-precipitation between TRPM8 and Gα_q was also observed in native DRG neurons (Fig. 6c). Both the N- and C-terminal domains of TRPM8 bind to Gα_q and to Gα_q Q209L, though stronger binding was observed to the N terminus (Fig. 6d). Neither Gα_{i2} nor Gαs showed significant binding to TRPM8 under similar conditions (Supplementary Fig. S5a-c). Furthermore, neither BK nor histamine promoted binding of Gα_q to TRPM8 (Fig. 6e). Thus Gα_q and TRPM8 form a constitutive complex, and activation of Gα_q by a GPCR does not enhance binding.

We next delineated the functional TRPM8 binding region on Gα_q by making a series of chimeras between active forms of Gα_q, which binds to and activates TRPM8, and Gα_i, which does not (shown schematically in Fig. 6f). All chimeras were similarly expressed, and none affected TRPM8 expression (Supplementary Fig. S5d,e). Chimeras Gα_{qi} and 2Gα_{qi} activated PIP_2 hydrolysis in a similar manner to Gα_q Q209L. However, 3Gα_{qi} lacked the ability to hydrolyse PIP_2 (Supplementary Fig. S4a), showing that the PLCβ binding region on Gα_q is located between E245 and Y261, in agreement with other findings[26]. Interestingly, this chimera still inhibited TRPM8 inward and outward currents, but a progressive loss of inhibition was found in chimeras 4Gα_{qi} and 5Gα_{qi} (Fig. 6f), and a corresponding loss of binding to TRPM8 was observed with the same deletions (Supplementary Fig. S5d), indicating that the region between N221 and N245 on Gα_q contains the functional TRPM8 binding region required for the modulation of TRPM8. This region corresponds to the Switch III helix region of Gα_q, which is structurally one of the most mobile regions and has extensive contacts with effectors. A modelled structure of heterotrimeric G$\alpha_q\beta\gamma$ indicates that the Switch III loop protrudes out of the protein surface and is free to be engaged by effectors such as TRPM8 (Supplementary Fig. S6). TRPM8 and PLCβ therefore bind to distinct but contiguous regions on Gα_q, rendering their mutual and independent regulation by Gα_q possible.

Activated Gα_q directly inhibits TRPM8 in excised patches

If activated Gα_q protein inhibits TRPM8 without the intervention of downstream signalling pathways, then the inhibition should be detectable in excised TRPM8-containing patches. TRPM8 channel activity runs down immediately after excision due to rapid loss of PIP_2[14, 15], but channels then remain active at a constant low level. Subsequent application of a water-soluble DiC8-PIP_2 restored channel activity to an even higher level (Supplementary Fig. S7a). We applied purified Gα_q protein, activated by prior incubation with GTPγS, to the intracellular surface of excised patches when channel run down was complete and activity had become stable. Activated Gα_q rapidly reduced the TRPM8 open probability (Supplementary Fig. S7b), an effect which could be due to activation of residual PLCβ trapped in the patch, and a consequent further reduction in levels of PIP_2. We found, however, that the inhibition of TRPM8 by activated Gα_q was even more prominent in the presence of saturating levels of DiC8-PIP_2, which strongly activates TRPM8 (Fig. 7a,b). In control experiments, application of Gα_q incubated with GDPβS, which forces Gα_q into the

inactive state, of boiled $G\alpha_q$, of $G\beta\gamma$, or of the activation buffer without GTPγS or $G\alpha_q$, were all without effect (Fig. 7e).

We showed above that $G\alpha_q$ constitutively binds to TRPM8. Endogenous $G\alpha_q$ should therefore remain in excised patches, associated with TRPM8, and should inhibit TRPM8 when switched into an active state. Consistent with this idea, addition of non-hydrolysable GTPγS, but not GDPβS, to inside-out membrane patches reduced the TRPM8 open probability both in the presence or absence of exogenous DiC8-PIP2 (Fig. 7c-e; Supplementary Fig. S7c). In experiments on patches excised from MEF cells lacking endogenous $G\alpha_{q/11}$ the application of activated $G\alpha_q$ itself inhibited TRPM8 as in patches from HEK293 cells, but the inhibitory effect of GTPγS alone was absent (Fig. 7e), confirming that $G\alpha_q$ remaining in the patch is indeed responsible for TRPM8 inhibition. This experiment also shows that subunits other than $G\alpha_{q/11}$ are not able to inhibit TRPM8 following activation by GTPγS.

DISCUSSION

Three mechanisms for modulation of ion channels by GPCRs have been well established. Channels can be modulated by phosphorylation by kinases such as PKA, PKC or Src[28, 29], by direct binding to $G\beta\gamma$ subunits released following GPCR activation[30, 31], or by interaction with membrane PIP_2[32-35]. We provide here evidence for a fourth mechanism: the $G\alpha_q$ subunit binds directly to TRPM8, and the conformational change of $G\alpha_q$ following GPCR activation causes a rapid and direct trans-inhibition of TRPM8 (Fig. 7f). It is tempting to speculate that the $G\alpha_q$ subunit could be involved in the regulation of other ion channels, a possibility that can now be investigated by the use of our $3G\alpha_{qiq}$ chimera, which allows unequivocal discrimination of a direct action of activated $G\alpha_q$ from downstream actions triggered by the PLC signalling pathway.

Previous studies have demonstrated that PIP_2 is a potent activator of TRPM8[14-16]. A decrease in membrane PIP_2 following activation of a Gq-coupled GPCR could therefore be responsible for inhibiting TRPM8. In the present study we confirmed that activation of Gq-coupled GPCRs caused a marked PIP_2 depletion. Unexpectedly, our evidence argues against a major physiological role for PIP_2 depletion in TRPM8 inhibition, because inhibiting PLC had little effect on TRPM8 inhibition following activation of Gq-coupled GPCRs, whereas a $G\alpha_q$ construct completely decoupled from PLC still had a strong action. Therefore, direct inhibition by activated $G\alpha_q$ causes the major part of the inhibition. A likely explanation for the lack of involvement of PIP_2 is that following activation of a G_q-coupled GPCR, TRPM8 is rapidly engaged and inhibited by activated $G\alpha_q$ even before the downstream PLCβ signalling pathway is initiated, so that subsequent PIP_2 depletion cannot further inhibit the channels. Another possibility is that the binding affinity of TRPM8 channels for PIP_2 is high, so that channels remain fully occupied by PIP_2 even when PIP_2 have been depleted by activation of PLC[32, 35].

We found that $G\alpha_q$ binds to TRPM8 even when inactive, and that binding was not enhanced by activation of $G\alpha_q$. It is likely that inactive $G\alpha_q$ binds to TRPM8 at an interface which differs from that of activated $G\alpha_q$, and that a conformational change upon activation causes a reorientation of $G\alpha_q$ to interact with a different site on TRPM8. We base this proposal on the observation that in isolated membrane patches, application of activated $G\alpha_q$ is able to inhibit TRPM8, even though TRPM8 is already bound to endogenous inactive $G\alpha_q$. $G\alpha_q$ thus functions as an integral component of the TRPM8 gating machinery, controlling the opening of TRPM8 channels and allowing rapid and efficient signal transduction. A similar association is also observed between G α_q and PLCβ, which form a preassembled complex[36], and in which activation of $G\alpha_q$ does not increase the association with PLCβ[37].

A recent study has also reported an interaction between TRPM8 and $G\alpha_q$[38]. This study showed that activation of TRPM8 causes downstream activation of the $G\alpha_q$-PLC metabotropic pathway. This effect is in the reverse direction to the $G\alpha_q$-to-TRPM8 inhibition demonstrated in the present paper, and raises the possibility that not only can $G\alpha_q$ influence the gating of TRPM8, as shown here, but that the gating of TRPM8 may also influence $G\alpha_q$. Activation of TRPM8 could in this scenario activate $G\alpha_q$, which would then inhibit TRPM8. In the absence of external Ca^{2+}, however, there is little rebound inhibition of TRPM8 currents following activation by menthol (see for example Fig. 4a), suggesting that any activation of $G\alpha_q$ by TRPM8 plays only a minor role in the gating of TRPM8.

The sensory information provided by cold-sensitive receptors is involved in the conscious sensation of coolness, in the detection of skin-surface dryness and in cold allodynia[11, 19]. The evidence that inflammatory mediators can inhibit the activity of cold-sensitive nerve terminals by a direct action of $G\alpha_q$ on TRPM8 has relevance for the understanding of cold disesthesias associated with injury and inflammation. Elucidating the molecular mechanism involved in the modulation of cold-evoked activity under inflammatory conditions opens up new possibilities for its selective therapeutic manipulation.

METHODS

Single unit recordings

Corneal nerve fibre recording was performed as described previously[19]. Briefly, eyes of adult C57BL/6J mice were removed and placed in a recording chamber perfused with the saline solution. A fire-polished glass recording pipette filled with physiological saline was applied to the surface of the corneal epithelium with slight suction to make extracellular recordings of nerve activity. Signals were amplified with an AC amplifier and data were captured and analyzed using a CED 1401 interface coupled to a computer running Spike2 6.0 software.

Tongue nerve fibre recording was performed in isolated tongues from adult male C57BL/6J mice. The tongue was removed from the head and right and left lingual nerves were isolated. The tongue was then transferred to a recording chamber continuously perfused with saline solution at 35°C. The distal end of one of the lingual nerves was placed in an adjoining compartment filled with paraffin oil and split into smaller filaments. A filament was placed on a monopolar platinum wire electrode connected to an amplifier to record impulse activity. When a filament displaying spontaneous activity was detected, a cold ramp down to around 10°C was delivered. Nerve filaments showing multiunit background discharge with cooling were further divided until a nerve filament containing a single or few active units was obtained. To induce an acute inflammation in the tongue, animals were injected with lambda carrageenan (2% in saline, 5μl) down the midline towards the tip of the underside of the tongue. This caused a marked tissue edema that was fully developed two hours later. The mouse was then sacrificed, the tongue was prepared and recorded in the same manner as above.

Cell culture and transfection

HEK 293 cells and MEF cells were maintained in DMEM medium containing 10% fetal bovine serum, 100 UI/ml penicillin, 100 μg/ml streptomycin and 2.0 mM L-Glutamine. For electrophysiology, HEK 293 cells were transiently transfected using polyfect transfection reagents (QIAGEN) according to manufacturer's instructions. MEF cells were transfected by using cell line nucleofection kits (Lonza). Electrophysiology recordings were typically performed 2~3 days following transfection. For molecular biology experiments, we use TurboFect transfection reagent (Fermentas).

DRG neuron isolation and culture were conducted as described previously[4, 5].

Molecular biology

cDNA constructs: Human $G\alpha_{q/11}$, $G\alpha_{i2}$, $G\beta_1$, $G\gamma_2$, $G\alpha s$, $G\alpha_{13}$ and H1R receptor cDNAs were purchased from Missouri S&T cDNA Rescource Center. GST coupled TRPM8 N and C terminal fragments and all $G\alpha_q$ chimers were constructed by standard PCR procedures. TRPM8 tagged with V5 and hexahis epitopes at C terminal were described as previously[5]. Mutagenesis was performed by using Quick-Change site-directed mutagenesis kit (Stratagene).

Pull down assays and co-immunopreciptation: To pull down hexahistidine-tagged TRPM8 with nickel beads, HEK293 cells transfected with TRPM8-V5-His and $G\alpha_q$ were solubilised in a lysis buffer consisting of 20mM HEPES, 1.0% NP40, 150mM NaCl, 0.4mM EDTA and 20mM imidazole plus protease inhibitor cocktail (Roche). Ni-NTA agarose beads (QIAGEN) were then incubated with cell lysate at 4°C followed by extensive wash with the lysis buffer. For GST pull down, c. 0.2μg purified GST coupled N (1~691) and C terminal (980~1104) protein fragments from BL-21 cells were incubated with either purified $G\alpha_q$ protein or cell lysate overexpressing G α_q/$G\alpha_q$ Q209L at 4°C for 3 hours, followed by overnight incubation with GST-agarose and centrifugation. For cross-linking experiments in Fig. 6e, treated HEK293 cells were incubated with 2.0mM cell permeable DSP (Dithiobis[succinimidyl propionate], Pierce) cross linker for 30 minutes before solubilisation and co-immunoprecipitation. All washed beads were boiled in sample buffer and loaded on 10% SDS-PAGE gel for western blot analysis. Coimmunoprecipittion was performed as described previously[4, 5]. For co-immunoprecipitation from DRG neurons in Fig. 6c, TRPM8 antibody (Transgenic Inc, Japan, KM060, 1:100) was used to precipitate TRPM8 in DRG neurons, and associated $G\alpha_q$ was detected by monoclonal anti-$G\alpha_q$ (Santa Cruz, sc-136181, 1:1000). Polyclonal anti-$G\alpha_q$ antibody (Santa Cruz, sc-393, 1: 2000) which recognizes $G\alpha_q$ N terminal domain was used for the detection of $G\alpha_q$ and all chimeric $G\alpha_q$ proteins. Antibodies against $G\alpha_{i2}$ (sc-13534, 1:2000) and $G\alpha s$ (sc-46975, 1:2000) were from Santa Cruz. All blots repeated at least three times with similar results.

Electrophysiology

Electrophysiological experiments were performed in calcium free bath solution unless otherwise stated to prevent desensitization of TRPM8.

Whole cell patch recording was performed largely as described previously[5]. Briefly, patch electrodes were pulled from thin walled glass capillaries, and had a resistance of 3.0~4.0MΩ when filled with internal solution with the following composition (in mM): 140 KCl, 2.0 $MgCl_2$, 5.0 EGTA, 10 HEPES, PH 7.4 with KOH. Cells were perfused with calcium free bath solution containing (in mM): 140 NaCl, 4 KCl, 10 HEPES, 1 $MgCl_2$, 5 EGTA, 5 glucose, pH 7.4 with NaOH. For experiments using calcium containing bath solution, EGTA was replaced with 1.8mM $CaCl_2$. TRPM8 inward and outward currents were measured at a holding potential of −60mV and +60mV, respectively. Cells were pre-treated with 1μM bradykinin or 10μM histamine for 1minute before break-in to the whole cell mode to measure TRPM8 currents activated by menthol. To examine TRPM8 activation by depolarization, steps of voltage pulses were applied for 100ms ranging from −140mV to +200mV in 20mV increments, followed by a final step to +60mV. Half maximal activation voltage ($V_{1/2}$) was obtained as described previously[5] by fitting normalized channel conductance (G/G_{max})-voltage relationship to a Boltzmann equation: $G/G_{max}=1/(1+\exp[-(Vm-V_{1/2})/k])$. All recordings were made at room temperature (24°C) with an Axopatch 200B patch clamp amplifier (Axon) in conjunction with pClampex 10.2 version software (Molecular Devices). Signals were analog filtered using a 1 kHz low-pass Bessel filter.

Cell attached and inside-out recordings were made using pipettes fabricated from thick wall borosilicate glass tubing (Sutter Instrument) with a resistance of 9~15 MΩ when filled with pipette solution. Pipettes were fire polished using a microforge and coated with Sigmacote(Sigma). For inside-out recordings we used a pipette solution with the following composition (in mM):140 NaCl, 3 KCl, 10 HEPES, pH7.3 with NaOH. Bath solution contained (in mM): 140 KCl, 5 EGTA, 1 MgCl2, 10 HEPES, 5 glucose PH7.3 with KOH. Menthol (500μM) was included in the pipette solution to activate TRPM8 channels within the patch. Recordings were sampled at 5 kHz and filtered at 2.0 kHz. For experiments in Fig. 7a, b, 50μM DiC8-PIP_2 (Echelon Biosciences) was present in the bath solution to prevent TRPM8 channel run-down. Activated G proteins were pulsed onto the excised patches through an ejection pipette positioned close to the patches. Ejection pipettes were connected to a PicoSpritzer III ejection system using nitrogen as a pressure source. Single channel data were analyzed using Clampfit10.2 software (Molecular Devices). Overall channel activities of patches (NP_o) were obtained by using the "50% threshold criterion" from the idealized traces[39]. All events were carefully checked visually before being accepted. For representation purposes traces were filtered at 500Hz.

G Protein purification and activation

$G\alpha_q$ protein was expressed and purified as described[40]. Briefly, human $G\alpha_q$, $G\beta_1$ and hexahis tagged $G\gamma_2$ were subcloned into transfer vector PVL1392. Each was cotransfected into Sf9 cells together with baculovirus flashback GOLD expression vector, and recombinant baculoviruses containing G protein subunits were amplified. Sf9 cells were then infected with a combination of those baculoviruses at a M.O.I of 3.0. Cells were harvested 48h after infection and solubilised by 1% sodium cholate. Proteins were purified by Ni-NTA agarose column followed by extensive washing. $G\alpha_q$ subunit was eluted from the column by 30μM $AlCl_3$ and subsequently purified by HiTrap Q HP anion exchange column (GE Healthcare). Proteins were eluted with a gradient of NaCl, peak fractions were collected and assayed by immunoblot with anti-$G\alpha_q$ antibody. Fractions containing the $G\alpha_q$ protein were pooled and concentrated to 0.3mg/ml using an Amicon Ultra filter and stored in aliquot of 3.0 μl at −80°C.

$G\alpha_q$ protein aliquots were activated in the presence of 0.2mM DTT, 1mM $GTP_\gamma S$ and 0.01% CHAPS in the patch bath solution at 30°C for 50 minutes. To remove excess $GTP_\gamma s$ after activation of $G\alpha_q$, the buffer for activated $G\alpha_q$ protein was exchanged by repeated dilution with bath solution and centrifugation by using an AmiconUltra fiter. Similar procedures were followed for deactivating $G\alpha_q$ with GTPβS.

We also purchased purified human $G\alpha_q$ protein from Origene, both sources of purified $G\alpha_q$ protein showed a similar effect. Purified bovine brain $G\beta\gamma$ subunits were obtained from Merck Biosciences.

Fluorescence imaging

Calcium imaging was performed at room temperature as described previously[4]. Briefly, transfected HEK293 cells or DRG neurons were plated onto a coverslip and loaded with Fluo-4-AM (Invitrogen). Cells were continuously perfused with normal Hanks solution and images were collected every 3s using a Bio-Rad confocal microscope. Pulses of menthol (100μM) were applied for 15 seconds every 4 minutes. Bradykinin (BK, 1μM) was applied for 2 minutes between the 5^{th} and 6^{th} menthol response. The effect of BK was quantified as a response ratio by dividing the 6^{th} by the 5^{th} peak response amplitude. In control experiments on cells not exposed to BK the distribution of response ratios was found to be well fitted by a normal distribution (supplementary Fig. S1d), from which a threshold ratio

was derived at 95% confidence level and used to determine cells significantly inhibited by BK.

Tubby-R332H-cYFP and PLCδ-PH-EGFP translocation was determined by live-scanning using a Leica confocal microscopy. Images of MEF cells transfected with the fluorescence probe, B2R and G proteins as appropriate were collected every 0.75s. Probe translocation was quantified by calculating the ratio of membrane fluorescence to that of cytosol using ImageJ software.

Statistics

All data are mean ± SEM. Difference between groups were assessed by either paired (Fig. 1a, 3a,b) or unpaired Student's *t* test (Fig. 5d, f and Supplementary Fig S3b), or by one way analysis of variance (ANOVA) with Bonferroni's *post hoc* test (for all other figures). Results were considered significant at $P<0.05$.

Supplementary Material

Refer to Web version on PubMed Central for supplementary material.

Acknowledgments

We thank Dr. S. Offermanns for providing MEF cells, Dr. G. Hammond for Tubby-R332H and PLCδ-PH-EGFP cDNA and for help with imaging analysis, Dr. O. Opaleye for help with protein purification, Dr. R. Hardie and Dr. S.B. Hladky for help with single channel recording, and Dr. R. Hardie for critical reading of an earlier version of the manuscript. This work was supported by an MRC new investigator research grant (G0801387 to X.Z.), a BBSRC research grant (BB/F003072/1to P.A.M.) and a grant from the BBVA (to P.A.M. ., to support a BBVA visiting professorship at the Instituto de Neurociencias, Alicante).

REFERENCES

1. Cesare P, McNaughton P. A novel heat-activated current in nociceptive neurons and its sensitization by bradykinin. Proc. Natl. Acad. Sci. U. S. A. 1996; 93:15435–15439. [PubMed: 8986829]
2. Numazaki M, Tominaga T, Toyooka H, Tominaga M. Direct phosphorylation of capsaicin receptor VR1 by protein kinase Cepsilon and identification of two target serine residues. J. Biol. Chem. 2002; 277:13375–13378. [PubMed: 11884385]
3. Bhave G, et al. Protein kinase C phosphorylation sensitizes but does not activate the capsaicin receptor transient receptor potential vanilloid 1 (TRPV1). Proc. Natl. Acad. Sci. U. S. A. 2003; 100:12480–12485. [PubMed: 14523239]
4. Zhang X, Huang J, McNaughton PA. NGF rapidly increases membrane expression of TRPV1 heat-gated ion channels. EMBO J. 2005; 24:4211–4223. [PubMed: 16319926]
5. Zhang X, Li L, McNaughton PA. Proinflammatory mediators modulate the heat-activated ion channel TRPV1 via the scaffolding protein AKAP79/150. Neuron. 2008; 59:450–461. [PubMed: 18701070]
6. Peier AM, et al. A TRP channel that senses cold stimuli and menthol. Cell. 2002; 108:705–715. [PubMed: 11893340]
7. McKemy DD, Neuhausser WM, Julius D. Identification of a cold receptor reveals a general role for TRP channels in thermosensation. Nature. 2002; 416:52–58. [PubMed: 11882888]
8. Proudfoot CJ, et al. Analgesia mediated by the TRPM8 cold receptor in chronic neuropathic pain. Curr. Biol. 2006; 16:1591–1605. [PubMed: 16920620]
9. Dhaka A, et al. TRPM8 is required for cold sensation in mice. Neuron. 2007; 54:371–378. [PubMed: 17481391]
10. Colburn RW, et al. Attenuated cold sensitivity in TRPM8 null mice. Neuron. 2007; 54:379–386. [PubMed: 17481392]

11. Chung MK, Caterina MJ. TRP channel knockout mice lose their cool. Neuron. 2007; 54:345–347. [PubMed: 17481385]
12. Daniels RL, McKemy DD. Mice left out in the cold: commentary on the phenotype of TRPM8-nulls. Mol. Pain. 2007; 3:23. [PubMed: 17705869]
13. Xing H, Chen M, Ling J, Tan W, Gu JG. TRPM8 mechanism of cold allodynia after chronic nerve injury. J. Neurosci. 2007; 27:13680–13690. [PubMed: 18077679]
14. Rohacs T, Lopes CM, Michailidis I, Logothetis DE. PI(4,5)P2 regulates the activation and desensitization of TRPM8 channels through the TRP domain. Nat. Neurosci. 2005; 8:626–634. [PubMed: 15852009]
15. Liu B, Qin F. Functional control of cold- and menthol-sensitive TRPM8 ion channels by phosphatidylinositol 4,5-bisphosphate. J. Neurosci. 2005; 25:1674–1681. [PubMed: 15716403]
16. Varnai P, Thyagarajan B, Rohacs T, Balla T. Rapidly inducible changes in phosphatidylinositol 4,5-bisphosphate levels influence multiple regulatory functions of the lipid in intact living cells. J. Cell Biol. 2006; 175:377–382. [PubMed: 17088424]
17. Premkumar LS, Raisinghani M, Pingle SC, Long C, Pimentel F. Downregulation of transient receptor potential melastatin 8 by protein kinase C-mediated dephosphorylation. J Neurosci. 2005; 25:11322–11329. [PubMed: 16339027]
18. Linte RM, Ciobanu C, Reid G, Babes A. Desensitization of cold- and menthol-sensitive rat dorsal root ganglion neurones by inflammatory mediators. Exp. Brain Res. 2007; 178:89–98. [PubMed: 17006682]
19. Parra A, et al. Ocular surface wetness is regulated by TRPM8-dependent cold thermoreceptors of the cornea. Nat. Med. 2010; 16:1396–1399. [PubMed: 21076394]
20. Cesare P, Dekker LV, Sardini A, Parker PJ, McNaughton PA. Specific involvement of PKC-epsilon in sensitization of the neuronal response to painful heat. Neuron. 1999; 23:617–624. [PubMed: 10433272]
21. Koike-Tani M, et al. Signal transduction pathway for the substance P-induced inhibition of rat Kir3 (GIRK) channel. J. Physiol. 2005; 564:489–500. [PubMed: 15731196]
22. Chen X, et al. Inhibition of a background potassium channel by Gq protein alpha-subunits. Proc. Natl. Acad. Sci. U. S. A. 2006; 103:3422–3427. [PubMed: 16492788]
23. Wu DQ, Lee CH, Rhee SG, Simon MI. Activation of phospholipase C by the alpha subunits of the Gq and G11 proteins in transfected Cos-7 cells. J. Biol. Chem. 1992; 267:1811–1817. [PubMed: 1309799]
24. Takasaki J, et al. A novel Galphaq/11-selective inhibitor. J. Biol. Chem. 2004; 279:47438–47445. [PubMed: 15339913]
25. Quinn KV, Behe P, Tinker A. Monitoring changes in membrane phosphatidylinositol 4,5-bisphosphate in living cells using a domain from the transcription factor tubby. J. Physiol. 2008; 586:2855–2871. [PubMed: 18420701]
26. Venkatakrishnan G, Exton JH. Identification of determinants in the alpha-subunit of Gq required for phospholipase C activation. J. Biol. Chem. 1996; 271:5066–5072. [PubMed: 8617784]
27. Offermanns S, et al. Embryonic cardiomyocyte hypoplasia and craniofacial defects in G alpha q/G alpha 11-mutant mice. EMBO J. 1998; 17:4304–4312. [PubMed: 9687499]
28. Yao X, Kwan HY, Huang Y. Regulation of TRP channels by phosphorylation. Neurosignals. 2005; 14:273–280. [PubMed: 16772730]
29. Huang J, Zhang X, McNaughton PA. Modulation of temperature-sensitive TRP channels. Semin. Cell Dev. Biol. 2006; 17:638–645. [PubMed: 17185012]
30. Clapham DE, Neer EJ. G protein beta gamma subunits. Annu. Rev. Pharmacol. Toxicol. 1997; 37:167–203. [PubMed: 9131251]
31. Dascal N. Ion-channel regulation by G proteins. Trends Endocrinol. Metab. 2001; 12:391–398. [PubMed: 11595540]
32. Gamper N, Shapiro MS. Regulation of ion transport proteins by membrane phosphoinositides. Nat. Rev. Neurosci. 2007; 8:921–934. [PubMed: 17971783]

33. Brown DA, Hughes SA, Marsh SJ, Tinker A. Regulation of M(Kv7.2/7.3) channels in neurons by PIP(2) and products of PIP(2) hydrolysis: significance for receptor-mediated inhibition. J. Physiol. 2007; 582:917–925. [PubMed: 17395626]
34. Nilius B, Owsianik G, Voets T. Transient receptor potential channels meet phosphoinositides. EMBO J. 2008; 27:2809–2816. [PubMed: 18923420]
35. Suh BC, Hille B. PIP2 is a necessary cofactor for ion channel function: how and why? Annu. Rev. Biophys. 2008; 37:175–195. [PubMed: 18573078]
36. Dowal L, Provitera P, Scarlata S. Stable association between G alpha(q) and phospholipase C beta 1 in living cells. J. Biol. Chem. 2006; 281:23999–24014. [PubMed: 16754659]
37. Grubb DR, Vasilevski O, Huynh H, Woodcock EA. The extreme C-terminal region of phospholipase Cbeta1 determines subcellular localization and function; the “b” splice variant mediates alpha1-adrenergic receptor responses in cardiomyocytes. FASEB J. 2008; 22:2768–2774. [PubMed: 18390926]
38. Klasen K, et al. The TRPM8 ion channel comprises direct Gq protein-activating capacity. Pflugers Arch. 2012
39. Studer M, McNaughton PA. Modulation of single-channel properties of TRPV1 by phosphorylation. J. Physiol. 2010; 588:3743–3756. [PubMed: 20693293]
40. Kozasa T, Gilman AG. Purification of recombinant G proteins from Sf9 cells by hexahistidine tagging of associated subunits. Characterization of alpha 12 and inhibition of adenylyl cyclase by alpha z. J. Biol. Chem. 1995; 270:1734–1741. [PubMed: 7829508]
41. Wall MA, et al. The structure of the G protein heterotrimer Gi alpha 1 beta 1 gamma 2. Cell. 1995; 83:1047–1058. [PubMed: 8521505]
42. Tesmer VM, Kawano T, Shankaranarayanan A, Kozasa T, Tesmer JJ. Snapshot of activated G proteins at the membrane: the Galphaq-GRK2-Gbetagamma complex. Science. 2005; 310:1686–1690. [PubMed: 16339447]

Europe PMC Funders Author Manuscripts

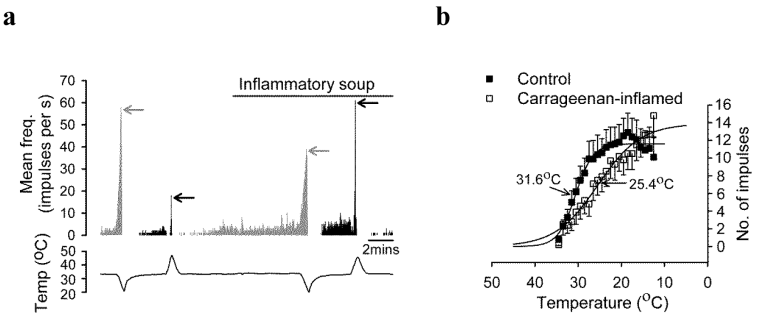

Figure 1.

Inflammatory mediators inhibit TRPM8-dependent cold nerve fibre activity. **(a)** Corneal nerve terminal firing frequency in response to a cold ramp (grey bars) and a heat ramp (black bars). Bath temperature shown below. Perfusion of "inflammatory soup" (5mM BK, 100mM histamine, 10mM PGE2, 100mM 5-HT and 100mM ATP) inhibited cold response (grey arrows) but enhanced heat response (black arrows). The cold response recovered to control levels following removal of IS (not shown) but heat response remained elevated. **(b)** Similar experiment on single afferent nerve fibres from tongue. Vertical axis shows cumulative firing during cold ramp. Filled squares: control (n=40); open squares: tongue injected with carrageenan (n=32, see Methods).

Europe PMC Funders Author Manuscripts

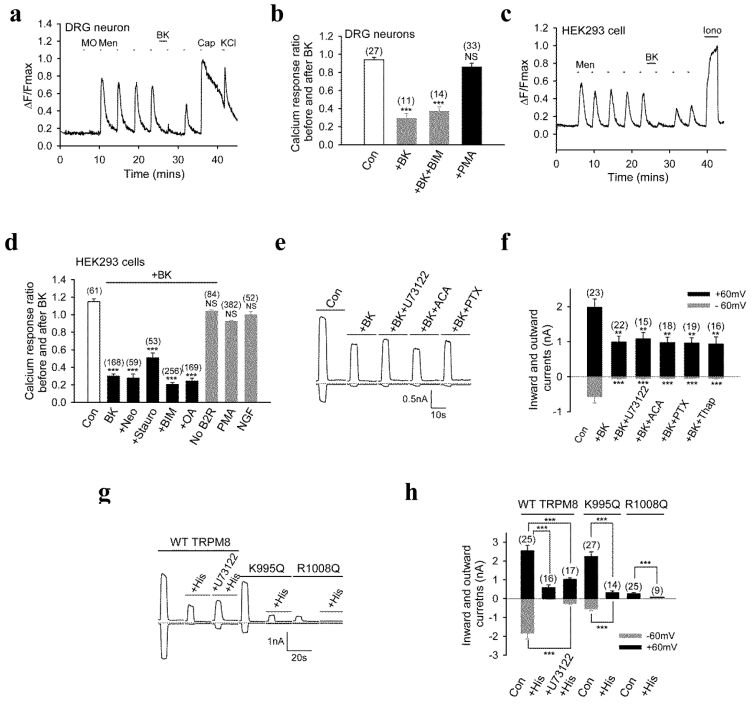

Figure 2.

Inflammatory mediators inhibit TRPM8 independent of downstream signalling pathways. **(a)** BK (1μM) inhibited TRPM8-mediated calcium response in a DRG neuron responding to menthol (100μM) and capsaicin (500nM) but not mustard oil (MO, 50μM), and thus expressing TRPM8 and TRPV1 but not TRPA1. KCl (140mM) added at end. **(b)** Summary of mean ratio of peak calcium responses to menthol before and after application of BK alone (bar 2), as in a, or with bisindolylmaleimide (BIM, 1μM) (bar 3). Bars 2 and 3 show only BK-responsive neurons but inhibition was also significant when BK-unresponsive cells included (Supplementary Fig. S1c). Final bar is summary of experiments with PMA (see Supplementary Fig. S1b). Number of TRPM8 positive neurons shown above each bar. **(c)** Ca increases elicited by menthol (100μM), and effect of BK (1μM) in a single HEK293 cell transfected with TRPM8 and B2R. Ca ionophore ionomycin (Iono,10μM) added at end to saturate Ca-dependent fluorescence. **(d)** Summary of results similar to those in c following treatment with: neomycin (neo, 1mM); Staurosporine (Stauro,1μM); Bisindolylmaleimide (BIM, 1μM); okadaic acid (OA, 20nM) and PMA (1μM) without BK. Final bar from cells transfected with TRPM8 and TrkA receptor, treated with NGF (100ng/ml, 10min). Number of cells given above each bar. **(e)** Inward and outward currents (at −60mV and +60mV) activated by menthol (200μM, 5s) in HEK cells expressing TRPM8 and B2R were inhibited by pre-treatment with 1μM BK (1min) applied alone or together with inhibitors as indicated. Dashed line denotes zero current. **(f)** Summary of peak currents in experiments similar to those in e following treatment with U73122 (2.5μM); N-(P-amylcinnamoyl)anthranilic acid (ACA, 10μM); pertussis toxin (PTX, 1.0μg/ml); thapsigargin (Thap, 1μM). Number of experiments given above each bar. **(g, h)** Example **(g)** and summary **(h)** of inward and outward currents (±60mV) in response to menthol (200μM, 5s) in HEK cells expressing TRPM8 or mutants as shown together with H1R. Histamine (His, 10μM) inhibits TRPM8 current, but little affected by 2.5μM U73122. Dashed line is zero current. Number of experiments given above each bar. All data are mean±SEM, significance compared to control. $^{**}P < 0.01$; $^{***}P < 0.001$; NS, not significant.

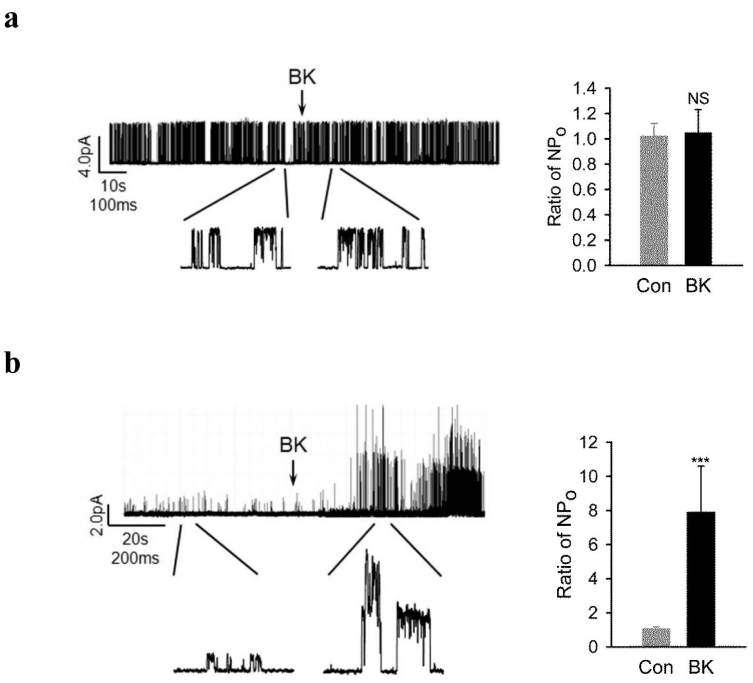

Figure 3.

Inhibition of TRPM8 by BK is membrane-delimited**. (a)** Typical cell attached recording of single channel at +60mV from HEK293 cells expressing TRPM8 and B2R. Arrow indicates addition of 1μM BK. Sections of traces shown below at a higher time resolution (see alternative scale bar on left). Mean NP_o before BK, 0.13 ± 0.0092; after BK, 0.14 ± 0.0093; difference not significant, $P > 0.05$. On right is summary of ratio of mean NP_o before and after vehicle solution (Con), and before and after BK from the same patches. n=5, NS, not significant. **(b)** Similar cell-attached recording performed at +40mV on a HEK293 cell expressing TRPV1 and B2R. Patch contains multiple channels. Mean NP_o before BK, 0.01711 ± 0.0014; after BK, 0.1866 ± 0.0243; $P < 0.001$. On right is summary of ratio of mean NP_o before and after vehicle solution (Con) or BK in the same patches. Enhancement by BK significant, ***$P < 0.001$, n=5. Error bars in all Figs are mean ± SEM.

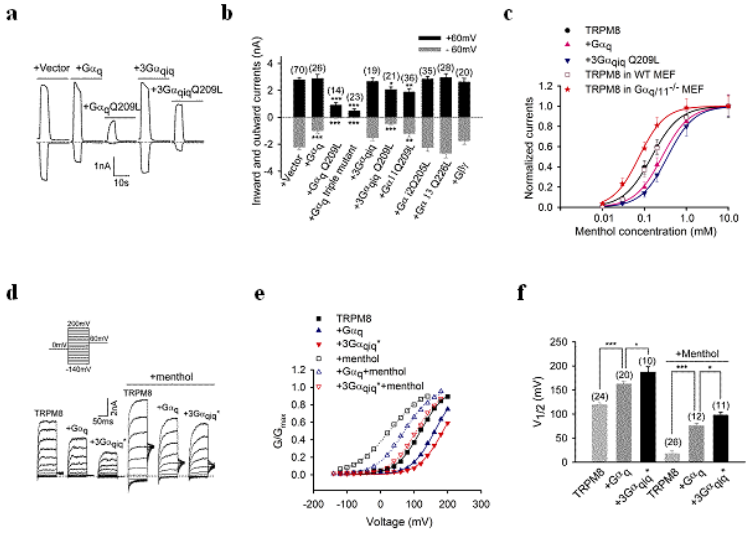

Figure 4.

Activated $G\alpha_q$ inhibits TRPM8 independent of PLC pathway. **(a)** Example of whole cell inward and outward currents (at −60mV and +60mV) activated by menthol (200μM, 5s) from HEK293 cells expressing TRPM8 and different $G\alpha_q$ mutants. Dashed line is zero current. **(b)** Summary of TRPM8 mediated inward and outward currents when transfected with different G protein subunits in experiments similar to those in a. "$G\alpha_q$ triple mutant" denotes $G\alpha_q$ Q209L/R256A/T257A. Number of experiments indicated above each bar. (**c**) Normalized whole cell inward currents at −60mV as a function of menthol concentration in HEK293 cells or MEF cells expressing TRPM8. Control dose-response curve in HEK293 cells (●), EC_{50}=148.8μM (n=8); cotransfection with $G\alpha_q$ (▲), EC_{50}=264.4μM (n=10); with $3G\alpha_{qiq}$ Q209L (▼), EC_{50}=356.1μM (n=9); wild type MEF cells (□), EC_{50}=156.8μM (n=5); $G_{\alpha q/11}^{-/-}$ MEF cells (★), EC_{50}=75.1μM (n=7). All curves show Hill equation with Hill coefficient of 1.31. (**d**) Representative TRPM8 currents elicited by voltage steps from −140mV to + 200mV (or to +140mV in the presence of 100 μM menthol) in 20mV increments in HEK 293 cells expressing TRPM8 and Gα proteins as indicated. Dashed line is zero current. $3G\alpha_{qiq}$* denotes activated Q209L mutant. Voltage-clamp protocol shown at top. **(e)** Conductance-voltage relationship for cells in d fitted by a Boltzmann function with values of $V_{½}$ and steepness factor as follows: TRPM8 alone (■), 119.4mV, 36.9mV; $+G\alpha_q$ (▲), 162.4mV, 35.1mV; $+3G\alpha_{qiq}$*(Q209L) (▼), 186.1mV, 36.3mV; +100μM menthol (□), 26.3mV, 52.1mV; $+G\alpha_q$+menthol (Δ), 71.7mV, 41.9mV; $+3G\alpha_{qiq}$*+menthol (▽), 107.3mV, 38.8mV. **(f)** Summary of $V_{½}$ values from experiments similar to those in d. Number of experiments given above each bar. All error bars are mean ± SEM. *P<0.05; **P<0.01; ***P <0.001.

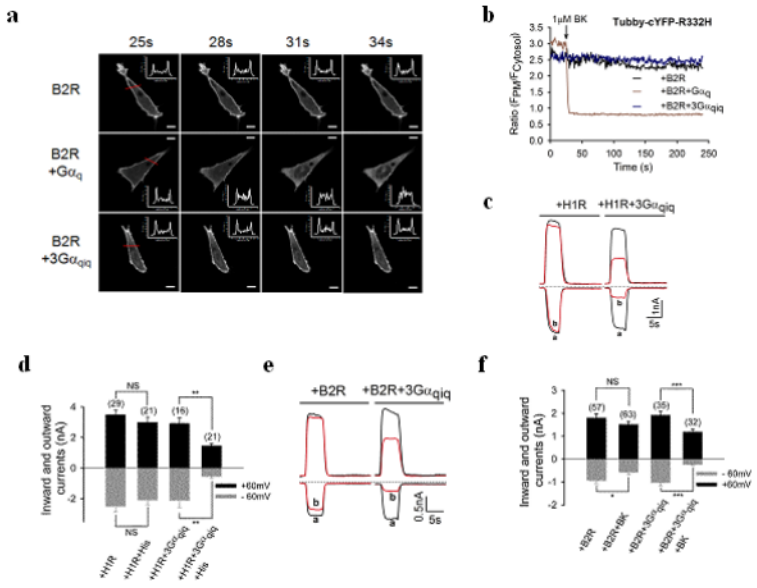

Figure 5.

Inflammatory mediators inhibit TRPM8 via a direct action of activated $G\alpha_q$. **(a)** Translocation of Tubby-cYFP-R332H induced by BK in $G_{\alpha q/11}^{-/-}$ MEF cells co-transfected with B2R and G proteins as indicated. 1μM BK was added at 25s. Scale bar 10μm. Profiles of intensity across cells (indicated by red line) shown inset at corner of the images. **(b)** Quantification of relative membrane Tubby fluorescence signal as a function of time in a. Each experiment repeated at least 4 times with similar results.**(c)** Typical traces of TRPM8 inward and outward currents (at −60mV and +60mV), activated by menthol (200μM, 5s) in $G_{\alpha q/11}^{-/-}$MEF cells transfected with H1R and TRPM8. Currents shown before (a) and after (b) histamine (10μM, 1min). Dashed line is zero current. **(d)** Summary of results similar to those in c. Number of experiments shown above each bar. All data are mean ± SEM. $^{**}P<0.01$; NS, not significant. **(e)** Similar experiments with application of BK (1μM) to $G_{\alpha q/11}^{-/-}$ MEF cells expressing B2R. **(f)** Summary of results similar to those in e. All bars are mean ± SEM. $^{*}P<0.05$; $^{***}P<0.001$; NS, not significant.

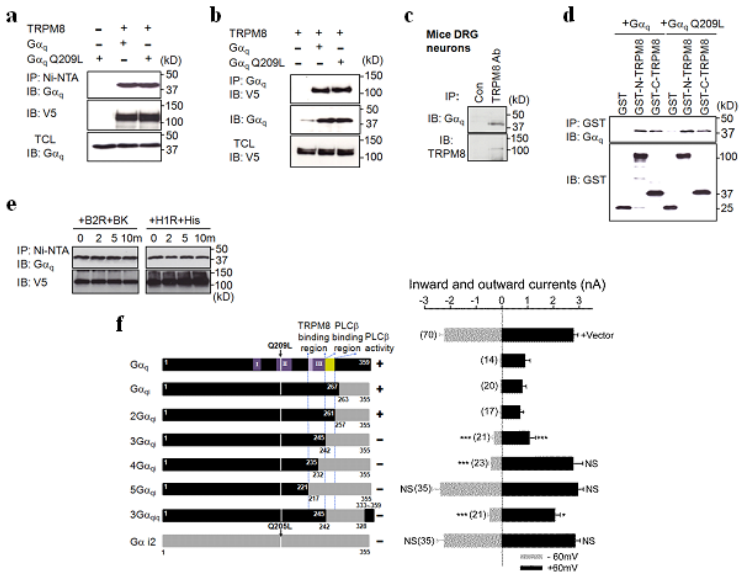

Figure 6.

Direct interaction of TRPM8 with $G\alpha_q$. **(a, b)** Mutual co-precipitation between TRPM8 and $G\alpha_q$. HEK293 cell lysate expressing TRPM8-V5-his and $G\alpha_q$/$G\alpha_q$ Q209L was pulled down by either nickel beads (a) or $G\alpha_q$ antibody (b), co-precipitated $G\alpha_q$ (a) or TRPM8 (b) was detected with indicated antibodies (top blots). Same blots stripped and reprobed with anti-V5 (a) or anti-G α_q (b) (middle blots). Bottom blots show similar $G\alpha_q$ (a) or TRPM8 (b) expression in total cell lysate (TCL) in all cases. **(c)** In DRG neurons $G\alpha_q$ was co-precipitated by TRPM8. Same blot reprobed with anti-TRPM8 (bottom). Specificity shown by omission of TRPM8 antibody from IP (Con, left lane). **(d)** $G\alpha_q$ and $G\alpha_q$ Q209L bind to TRPM8 N and C terminal. GST-coupled TRPM8 N and C terminal used to pull down cell lysate expressing $G\alpha_q$ or $G\alpha_q$ Q209L (top blot). N terminal binds 1.28±0.025 fold more $G\alpha_q$ than does C terminal (n=3). Blot stripped and reprobed with anti-GST (bottom). **(e)** Bradykinin and histamine did not enhance binding of $G\alpha_q$ to TRPM8. Cells expressing TRPM8-V5-His and B2R or H1R were treated with DSP after exposure to bradykinin (1μM, left) or histamine (10μM, right) for different minutes. TRPM8 pulled down by Ni-NTA, and the associated $G\alpha_q$ detected by anti-$G\alpha_q$ (top blot). Blots reprobed with anti-V5 (bottom). **(f)** TRPM8 binds to switch III region on $G\alpha_q$, resulting in the suppression of TRPM8. On left is schematic diagram of chimeras between $G\alpha_q$ Q209L (black bars) and $G\alpha_{i2}$ Q205L (grey bars). Number of amino acids in each protein used for the chimera given at the top corner of black bars ($G\alpha_q$ Q209L), or underneath grey bars (Gαi2 Q205L). Switch I, II and III regions on $G\alpha_q$ in purple, TRPM8 and PLCβ binding regions indicated by dotted blue lines. Ability of chimeras to activate PLCβ (Supplementary Fig. S4a) indicated to right of each chimera, +, activated; –, ineffective. Second bar from bottom shows construction of $3G\alpha_{qiq}$ in which distal C-terminal of G α_q (333-359) has been transplanted back into $3G\alpha_{qi}$ in order to allow coupling to G_q-coupled GPCRs. Right: summary of TRPM8 currents caused by chimeras shown on left. Number of experiments shown to left of each bar. Error bars, S.E.M. **P*<0.05; ****P*<0.001; NS, not significant. Uncropped images of blots (**6a-e**) shown in supplementary Fig.S8.

Europe PMC Funders Author Manuscripts

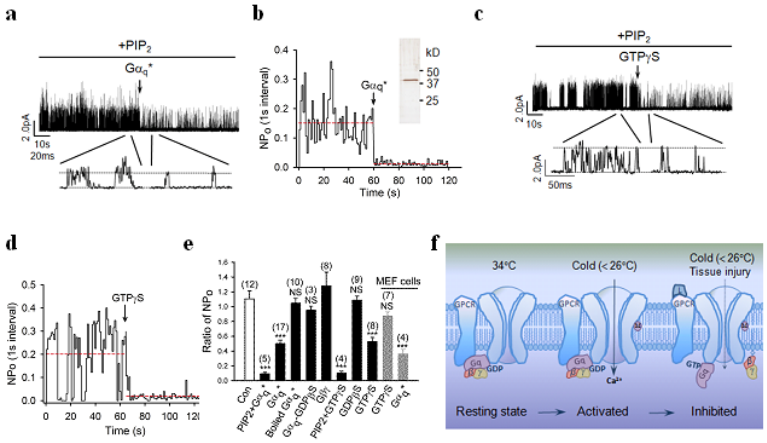

Figure 7.

Activated $G\alpha_q$ directly inhibits TRPM8 in excised patches**. (a)** Left: typical example of channel activity at +40mV in inside-out patches excised from HEK cells expressing TRPM8 after addition of 50nM $G\alpha_q$* ($G\alpha_q$ pre-incubated with GTPγS) in the presence of 50μM DiC8-PIP_2. Arrows indicate time of addition of $G\alpha_q$*. Sections of traces are shown below at higher time resolution. Note that single-channel currents are smaller than in Fig. 3a, because membrane potential was lower. **(b)** Real time quantification of NP_o in a. Red dashed lines give mean NP_o over indicated time period. Inset shows silver stain of purified $G\alpha_q$ protein. Mean NP_o before $G\alpha_q$*, 0.151 ± 0.0088; after $G\alpha_q$*, 0.013 ± 0.001; P<0.001. **(c)** Similar experiment to a, but with application of 100μM GTPγS. **(d)** Real time quantification of NP_o in c. Red dashed lines give mean NP_o over indicated time period. NP_o before GTPγS, 0.20±0.016; after GTPγS, 0.019 ± 0.0027; P<0.001; **(e)** Mean values of ratios of NP_o for treatments shown below bars (ratio is mean value over period 1minute after application, to that 1min before, see plots in b, d). Number of experiments given above each bar. All data are mean ± SEM. ***P<0.001 compared to control solution; NS, not significant relative to control. **(f)** Cartoon depicting proposed mechanism for regulation of TRPM8 by $G\alpha_q$ subunit. Left: in resting state at 34°C, TRPM8 is pre-bound to $G\alpha_q$. TRPM8 activity is low at this temperature. Middle: cold temperature or a cooling compound such as menthol (M) activates TRPM8, resulting in an inward current flow and an increase in firing frequency of cold fibres. Right: Inflammatory mediators (L) released by tissue injury bind to a GPCR resulting in GTP-GDP exchange and consequent activation of $G\alpha_q$. The consequent conformational change in Gαq causes inhibition of TRPM8 by a direct interaction, resulting in a decrease in current passing into the nerve terminal through TRPM8 and so a decreased firing of cold-sensitive nerve fibres.

Europe PMC Funders Author Manuscripts